Journal of Applied Polymer Science

Synthesis and properties of amphiprotic polyacrylamide microspheres as water shutoff and profile control

Zhisheng Yu, Yingcheng Li, Ou Sha, Zhiqing Su, Wenle Zhou
Sinopec Shanghai Research Institute of Petrochemical Technology, Shanghai 201208, People's Republic of China
Correspondence to: Y. Li (E-mail: liyc.sshy@sinopec.com)

ABSTRACT: Heat- and salt-resistant amphiprotic polyacrylamide microsphere (APMS) was synthesized using inverse microemulsion polymerization method. The microstructure, swellability, filtration, and core flooding performances were tested and characterized. FT-IR spectroscopy indicates that APMS was successfully prepared. Morphological analysis reveals that it is relatively uniform and spherical with an average diameter about 50 nm. Its average diameter increases up to 634 nm after aging at 90°C for 7 days in synthetic brine. After aging for 30 days, the particle size is decreased to 482 nm. But the swelling magnification is still 9.6 times its initial diameter. Compared with the traditional microspheres, APMS exhibits excellent thermal stability, salt resistance, and swelling properties. In addition, the plugging factor is in the range of 0.236 to 0.317, and the number of particles for bridge-plugging is slightly increased from 2 to 4 over aging time. Moreover, the plugging parameters show that APMS can favorably enter and effectively plug the artificial cores with permeability of 0.19 to 0.50 μm^2 by deformation, breakthrough and migration, bridging and plugging mechanisms. Furthermore, APMS also shows well its resistance to water flushing and good plugging strength in continuous injection experiment.
 J. Appl. Polym. Sci. **2016**, *133*, 43366.

KEYWORDS: core plugging; inverse micro-emulsion polymerization; polyacrylamide microspheres; salinity-resistant; swellability

Received 7 September 2015; accepted 21 December 2015
DOI: 10.1002/app.43366

INTRODUCTION

In recent years, many organic and inorganic materials are widely used in heterogeneous oilfield to control water and enhance oil recovery (EOR) through improving the water injection profiles at both academic and industrial levels.

As an important part of oilfield chemicals, water-soluble polymers and their compounds with alkali and surfactant for EOR applications have been successfully and extensively applied in oilfields.[1–4] However, polymers are degradable chemically, radically and thermally in the complicated and harsh conditions, exhibiting the weak heat-resistance, salt-resistance, and tolerance to shear properties.[5,6] On the other hand, the reservoir heterogeneity limits the application and efficiency of polymer flooding at a certain degree.

So, polymers with special structures or modified groups have been synthesized for enhanced oil recovery. Wever *et al.*[7] and Taylor and Nasr-El-Din[8] discussed the water-soluble hydrophobically associating polymers that had potential use in mobility control, drilling fluids and profile modification. In contrast to partially hydrolyzed polyacrylamide, these polymers exhibit excellent viscoelasticity, salinity-tolerance and viscosity thinning under shear.[9,10] Nonetheless, the solubility, critical concentration, and solution stability of the hydrophobically associating polymer are of great concern and need to be preferentially conquered.

At the same time, some researches with regard to gels for plugging and reducing fluid production were proposed and studied.[11,12] Because of the low selectivity of inorganic or nonpolymer gels on oil, the successful cases of construction is very rare. Later, some gel-based technologies have been developed for plugging fracture or high permeability strips.[13–20] Among them, the in-depth drive fluid diversion and the colloidal dispersion gel techniques broke the tradition and showed regulating action on in-depth fluid.[21,22] Even though, they have no defined shape and surface plugging can easily form, because of their large size. The influence of reservoir performances on gelation, the gel system harmful to formation, and the injection technology, etc, are also still unresolved issues.

Swellable crosslinking polyacrylamide microspheres are extensively applied for water shutoff, plugging, profile modification and in-depth fluid regulation in oilfield.[23,24] They can penetrate deeply into formation, deform and pass through fracture and block-off pore path.[25] This technology is mainly targeted at the reservoirs with serious heterogeneity, high water-cut and

Table I. Ionic Composition of Synthetic Formation Water

Composition content (mg L^{-1})	Na^+	Ca^{2+}	Mg^{2+}	Cl^-	TDS
	64,849	4000	1000	110,151	1.8×10^5

macroporous channels, and ultimately improving the development effect of water flooding and the final recovery of produced oil.

Previous studies showed that the size, distribution, and viscoelasticity of microspheres play an important role in plugging property.[26–30] Only in the context of a matched particle size with pore throat, the significant value of spheres applied in flooding emerges clearly. Besides, the capture-, superposition-, and bridge-plugging mechanisms occurred while elastic microspheres transferred and retained in porous media. And they could remigrate in pore-throats depending on their elasticity through four steps of capture-plugging, elastic deformation, steady migration, and deformation recovery.[25]

On the other hand, in order to improve the long-term effect and efficiency in rigorous environment, the microspheres with special structures and properties should be considered and designed. The particular structures contain long-branched chain, aromatic group, associated structure, and the group resistant to calcium and magnesium ions, etc. Besides, electrostatic attraction occurs between positive and negative ions. Net-like structure similar to pseudo crosslinking can be formed among the chains of amphiprotic polymer, which endows it with excellent performances.[31,32] As a consequence, all of those will bring out good combined performances of microspheres, for instance, strong interaction, resistance to heat, salinity, hydration and shear, and so on.

In this article, in order to develop one water shutoff and profile control agent for high temperature high salinity reservoir, we designed and synthesized a kind of heat- and salinity-resistant polyacrylamide microspheres with pendent aromatic rings, anionic and cationic groups via inverse microemulsion polymerization method. As well, the microsphere structure and swelling behavior were investigated and compared with a traditional polymer microsphere. The effect of aging time on the membrane filtration and the core plugging performance of microspheres were also evaluated for potentially long-term effective applications.

EXPERIMENTAL

Materials

Acrylamide (AM), 2-acrylamido-2-methylpropane-sulfonate (AMPS), 60 wt % water solution of dimethyl diallyl ammonium chloride (DMDAAC), and white oil obtained from Shandong Polymer Bio-chemicals Co., Ltd., China were industrial grade products and used without further purification. Tert-butyl styrene (TBS) purchased from Sinopharm Chemical Reagent Co., Ltd., China was industrial grade product and vacuum distilled over calcium hydride just before polymerization. Analytical grade potassium persulfate (PPS), sodium bisulfite (SBS), sodium acetate (SA), and *N*,*N*′-methylene bisacrylamide (MBA) obtained from Sinopharm Chemical Reagent Co., Ltd., China were reagent grade products and used as received. Reagent grade products, acrylic acid (AA, chemically pure), sorbitan monooleate (Span 80, chemically pure), and polyoxyethylene (20) sorbitan monostearate (Tween 60, chemically pure) were obtained from Sinopharm Chemical Reagent Co., Ltd., China and used without purification. Other reagents were obtained from Sinopharm Chemical Reagent Co., Ltd., China and used as received, such as ethanol, ethylenediaminetetraacetic acid sodium salt (EDTA-2Na), sodium hydroxide (NaOH), sodium chloride, magnesium chloride hexahydrate, and calcium chloride. They were all reagent grade products. The polyacrylamide microspheres (PAMS) applied in oilfield was supplied by Sinopec Zhongyuan Oilfield Branch, China. Deionized water was used for the preparation of all aqueous solutions. Composition of synthetic brine was shown in Table I.

Synthesis of Polymer Microspheres

Span 80 (23.4 g, 23.5 mL), Tween 60 (8.7 g, 8.3 mL), white oil (80.0 g, 97.6 mL), and TBS (2.6 g, 3.0 mL) were added to a 500 mL glass reactor fitted with a stirrer, a reflux condenser, a thermometer, and a nitrogen inlet tube at ambient temperature. The oil phase was prepared by thoroughly stirring. Water phase composed of deionized water (32.0 g, 32.0 mL), NaOH (3.6 g, 0.090 mol), AA (5.2 g, 5.0 mL), AM (36.2 g, 0.510 mol), AMPS (3.9 g, 0.019 mol), DMDAAC (6.5 g, 6.0 mL), SA (1.7 g, 0.021 mol), MBA (0.518 g, 3.364 mmol), and EDTA-2Na (0.020 g, 0.054 mmol) was prepared in a glass container. After adjusting its pH to 8 to 9 by sodium hydroxide aqueous solution with a concentration of 5%, the water phase were poured into the above oil phase. The mixture was stirred at 300 rpm for 20 min to obtain microemulsion. After purging with nitrogen for 15 min, the polymerization was initiated by drop-feeding PPS aqueous solution (3.0 g, a concentration of 4.3%) and SBS aqueous solution (3.0 g, a concentration of 3.5%) successively. After reacting for 0.5 h, the mixture was heated up to 50°C for 4h and a translucent microemulsion system was obtained. The as-prepared amphiprotic polyacrylamide microsphere is denoted by APMS. Its formula of copolymerization is shown in Figure 1. The solids content of APMS microemulsion was 25.20%, and the conversion of monomers was 95.21%. In contrast to APMS and PAMS, a biopolymer P(AM/AMPS) was synthesized using AM (51.8 g, 0.730 mol) and AMPS (3.9 g, 0.019 mol) under the same polymerization conditions.

Measurement and Characterization

Solids Content of Microemulsion. The microemulsion (m_0) was dispersed in threefold equivalent ethanol under vigorously stirring. After filtration, the filter cake was washed for three times with ethanol, and then dried in a vacuum oven at 50°C under 10^{-1} Pa for 12 h. The weight of the dried microsphere filter was marked as m_p. The solids content of microemulsion (S) was calculated by the following formula:

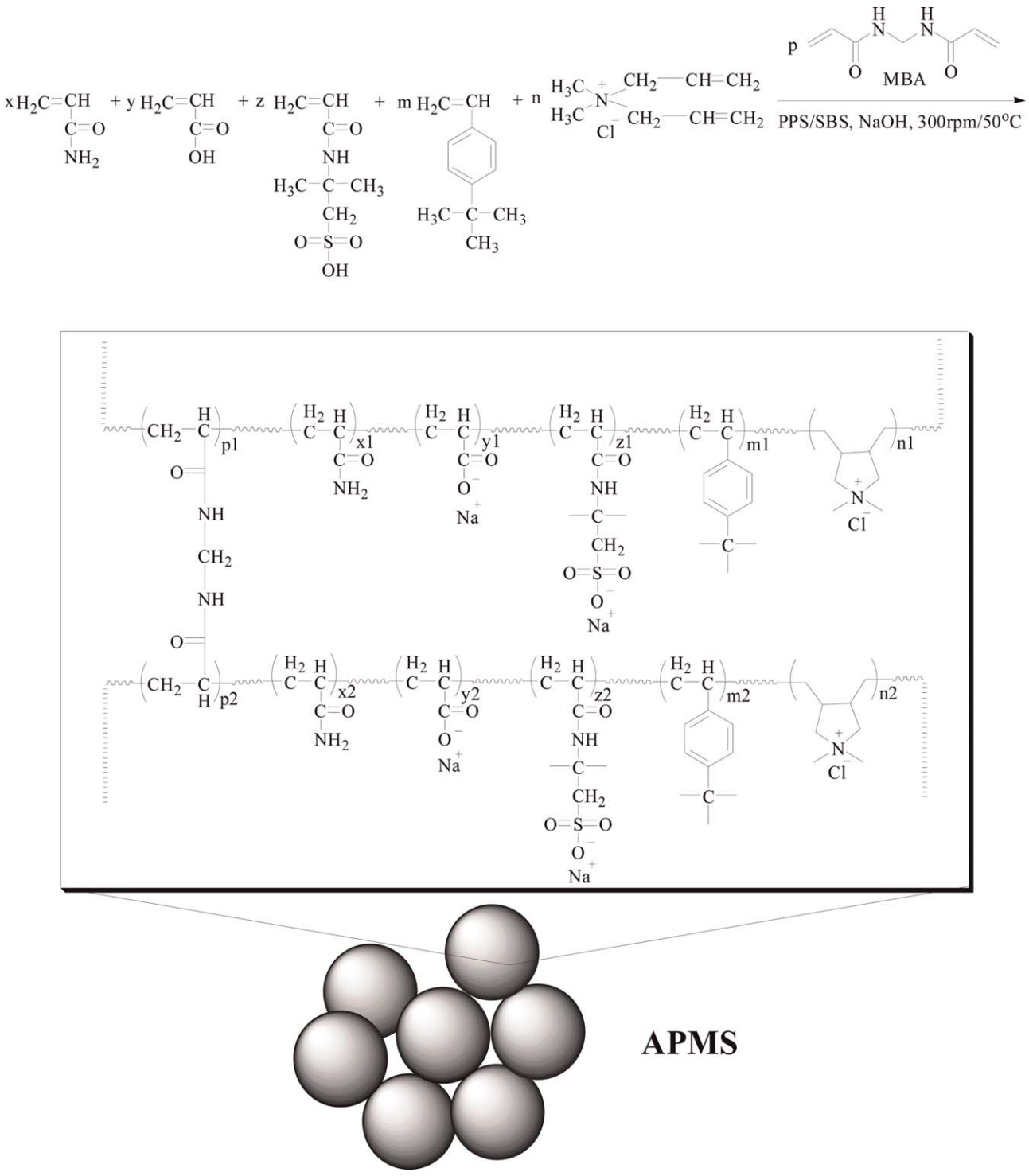

Figure 1. Formula of copolymerization of monomers.

$$S = \frac{m_p}{m_0} \times 100\%$$

Total Conversion of Monomers. The postprocessing method of microemulsion was same as mentioned above. The weights of AM, AA, AMPS, DMDAAC, TBS, and MBA were signed as m_a, m_b, m_c, m_d, m_e, and m_f, respectively. The weight of the obtained microspheres after copolymerization was marked as m_p. And AA and AMPS monomeric units existed in the form of sodium salt in the microstructure of copolymer. The total conversion of monomers (X) was calculated as follow:

$$X = \frac{m_p}{m_a + m_b \times \frac{94}{72} + m_c \times \frac{229}{207} + m_d \times 60\% + m_e + m_f} \times 100\%$$

FT-IR Spectroscopy. Infrared spectrum of polymer microspheres was examined by use of a Nicolet 20DXB

spectrophotometer (US) of 4000 to 400 cm^{-1} using 32 scans and 4 cm^{-1} of resolution.

^{1}H NMR Spectrometer. Nuclear magnetic resonance spectrum was measured by using a Bruker Avance 600 MHz ^{1}H NMR Spectrometer (CH). And the deuterated water was used as solvent.

Morphology and Particle Size. A Model XL30 scanning electron microscopy (SEM, Philips-FEI, NL) was adopted to observe the microsphere morphology. The original state and expanding particle size distribution were measured using a Zetasizer Nano-ZS90 dynamic laser particle size analyzer (Malvern Instrumented Ltd., UK). Three tests were performed for each sample at 25°C.

Swellability. After stirring for 2 h with a mechanical stirrer, the dried polymer microspheres were uniformly dispersed in synthetic brine water with a TDS of 1.8 × 10^5 mg L^{-1}. The solid concentration of microspheres was 0.05% by weight. After purging with nitrogen, the microspheres/brine solution was sealed in glass bottle and aged at 90°C in oven.

Membrane Filtration Testing. After swollen for different days under 90°C in synthetic brine water, the microspheres were carried out for filtration tests using the model device by installing with a microporous filtering membrane.[33] The micropore size and thickness of the membrane were 1.2 μm and 10.0 μm, respectively. The gas pressure applying on the microsphere solution was constantly 0.17 MPa.

Core Plugging Testing. The migration and plugging properties of microspheres in artificial cores with different permeability (0.19 μm^2, 0.50 μm^2) were measured according to the typical core-flooding apparatus.[34] The length and diameter of cores were 50 mm and 25 mm, respectively. Three procedures were totally performed: (1) inject synthetic brine with a TDS of 1.8 × 10^5 mg L^{-1} to get an initial pressure P_0; (2) inject microspheres suspension of 0.05% by weight and record an equilibrium pressure P_e; (3) inject brine with a TDS of 1.8 × 10^5 mg/L once again and record a maximum pressure P_m. All the procedures were performed in operation box under 90°C. The injection rate was fixed at 0.50 mL min^{-1} (6.12 cm h^{-1}). The resistance factor F_R and the residual resistance factor F_{RR} were calculated as follow, respectively.

$$F_R = \frac{P_e}{P_0}$$

$$F_{RR} = \frac{P_m}{P_0}$$

RESULTS AND DISCUSSION

Structure Characteristics

Figure 2 shows the typical FT-IR spectra of APMS, PAMS, and P(AM/AMPS). As shown in Figure 2(a), P(AM/AMPS) exhibits the strong absorption bands in the 3700 to 3100 cm^{-1} region because of the stretching vibrations of amine group (N–H). In addition, the broad absorption band near 1666 cm^{-1} is attributed to the stretching vibrations of carbonyl groups (C═O) belonging to amide and carboxyl groups. Also, there exists the moderate absorption bands at 1187 cm^{-1}, 1122 cm^{-1}, and

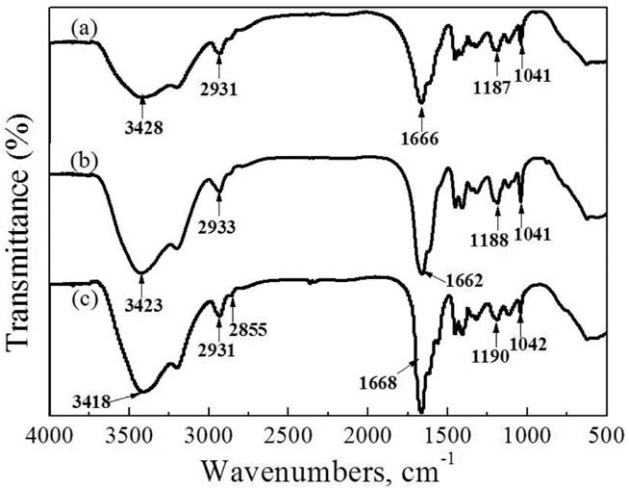

Figure 2. FT-IR spectra of (a) P(AM/AMPS), (b) PAMS, and (c) APMS.

1041 cm^{-1}, corresponding to the symmetric and asymmetric stretching vibrations of sulfonate ion (O═S═O).[35] The PAMS displays a same spectrum to P(AM/AMPS), expressing the absorption peaks of amine group and sulfonate ion [Figure 2(b)]. So it can be presumed that PAMS is a copolymer of AM and AMPS monomers. As for APMS, the absorption characteristics of DMDAAC, TBS and AA were covered due to the lower concentration or associated with other groups [Figure 2(c)].

The ^{1}H NMR spectrum was performed for further confirming the preparation and component of APMS. The relative spectrum, chemical shift and assignment of protons were shown in Figure 3 and Table II, respectively. Obviously, all the characteristic chemical shifts show that the amphiprotic polyacrylamide microspheres were successfully synthesized by the copolymerization of AA, AM, AMPS, DMDAAC, and TBS by molecular design.

The morphology of APMS is shown in Figure 4(a), where the particles are roughly spherical and relatively uniform. The mean particle size is approximately 50 nm and about half the size of PAMS used in the oilfield at present, which is about 90 nm as

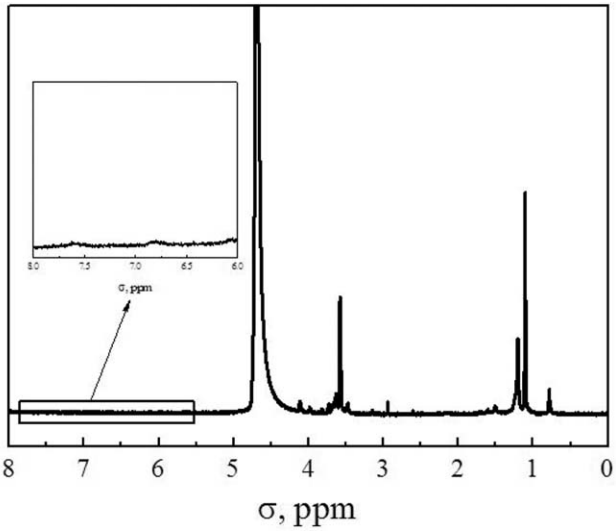

Figure 3. ^{1}H NMR spectrum of APMS.

Table II. ^{1}H NMR Results of APMS

Proton peak	δ (ppm)	Assignments
Unsaturated aromatics	7.6, 6.8	-CH=CH*- (TBS)
Deuterium reagent	4.9–4.3	O-D* (D_2O)
Saturated aliphatics	4.2–4.1	N-CH*- (AMPS)
	3.8–3.4	O-CH*-C (ethanol); N-CH*-C (DMDAAC)
	3.0–2.9	SO_3^--CH*-C (AMPS)
	2.6–2.5	=CH*-CH*-C (TBS)
	1.7–1.4	C-CH*-C (DMDAAC)
	1.3–1.0	C-CH* (ethanol); C-CH* (AA, AM, AMPS, TBS)
	0.8–0.7	C-CH* (AMPS, TBS, terminal methyl)

shown in Figure 4(b). P(AM/AMPS) shows a similar appearance morphology to PAMS and an average particle size near 75 nm which is slightly smaller than the latter [Figure 4(c)].

Swellability

The average particle size and distribution of microspheres before and after aging at 90°C in synthetic brine were measured. The average particle size and swelling magnification of PAMS, P(AM/AMPS) and APMS were investigated. The results were illustrated in Table III. Swelling magnification is defined as the ratio of the average particle size after absorbing water to the initial particle size estimated by SEM images. It is shown that PAMS can stably swell under the high temperature and salinity conditions for only 2 days. The average size is about 496 nm and 5.5 times larger than the original size. Afterwards, the cloudy white precipitates settle at the bottom of the glass bottle, which indicates that PAMS have poor heat resistance and salt tolerance, though it has 4.9 wt % of AMPS units resistant to divalent ions according to the quantitative analysis method.[36] The similar results were also obtained for P(AM/AMPS) with 7.0 wt % of AMPS units. The biopolymer microspheres would precipitate from the brine after 7 days under 90°C. So the followed characterizations containing filtration and plugging tests were not preformed any more for them.

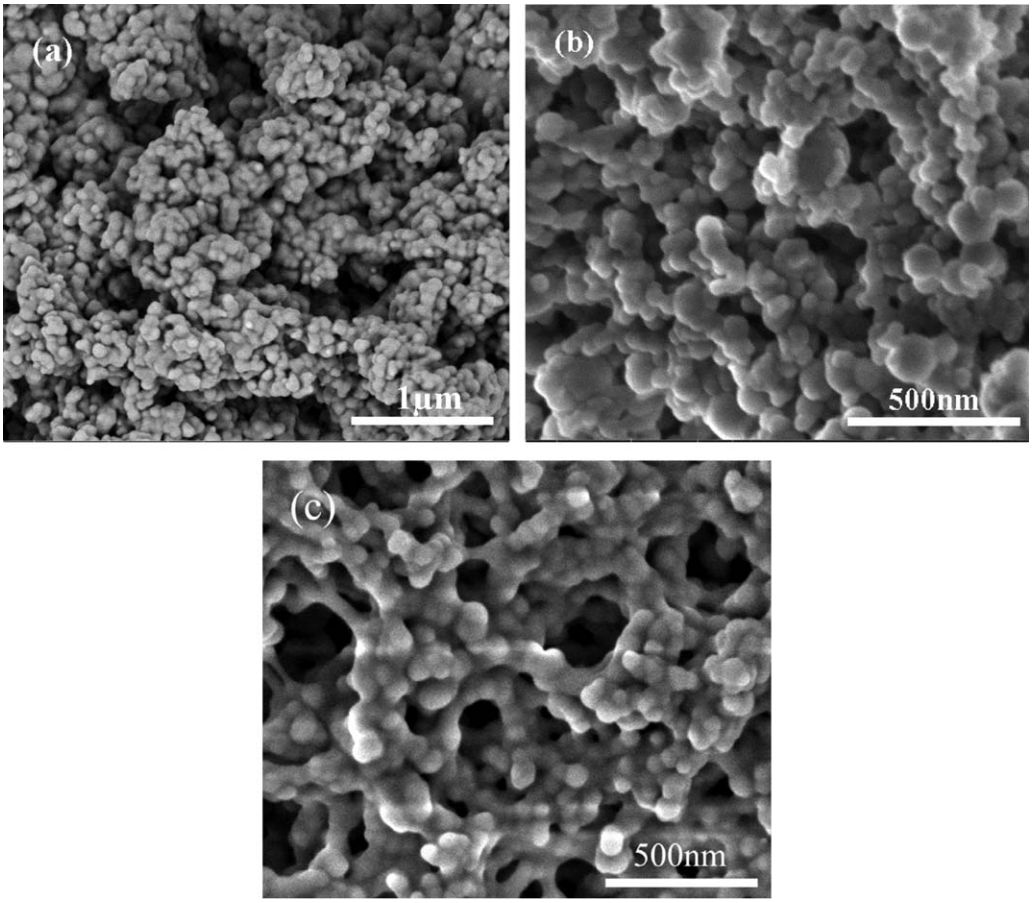

Figure 4. SEM micrographs of (a) APMS, (b) PAMS, and (c) P(AM/AMPS).

Table III. Results of Particle Size and Swelling Magnification of APMS, PAMS and P(AM/AMPS) after Aging

Swellability	APMS						PAMS			P(AM/AMPS)			
	Aging time (d)												
	0	2	7	14	21	30	0	2	≥3	0	2	7	≥7
Average particle size (nm)	50	435	634	555	465	482	90	496		75	676	812	
Particle size distribution	/	0.26	0.27	0.26	0.24	0.24	/	0.40	Precipitation	/	0.36	0.44	Precipitation
Swelling magnification	1.0	8.7	12.7	11.1	9.3	9.6	1.0	5.5		1.0	9.0	10.8	

In contrast, as presented in Figure 5 and Table III, APMS can quickly absorb water and expand under high salinity and high temperature conditions. The maximum average particle size is up to 634 nm after 1 week, and the swelling magnification is well over 12.7. The corresponding size volume fraction curves of APMS swollen for 7 days before and after filtration are illustrated in Figure 6. It shows the average particle size decreases from 634 nm to 280 nm and massive larger particles are trapped by membrane. Furthermore, the particle size is decreased and tends gradually to a relative balance after 3 weeks. The declined diameter is mostly due to the hydration of the outer layer of APMS. However, the swelling magnification is still higher than 9.0 after one month as well as the long-term stability, indicating that the as-prepared microspheres have excellent tolerance to divalent ions and restriction to hydrolysis at high temperature.

As for the heat resistance of APMS, it is largely ascribed to the existence of five-membered ring and aromatic ring structures. As for its salt tolerance, it is mainly because the sulfonate ion presents excellent tolerance to the divalent ions (e.g., calcium and magnesium ions) in brine. On the other hand, the well swellability for a long-term aging test can be attributed to the appropriate elasticity of crosslinking networks, Donnan potential due to the osmosis of counterions and the mixing entropy of macromolecular chains with water molecules, as explained in Flory-Huggins theory. Similar phenomena for the poly(acrylic acid-*co*-acrylamide) and poly(acrylamide-methylacryloxylethyl trimethyl ammonium chloride) microgels were also reported by Kiatkamjornwong and Phunchareon and Li *et al.*, respectively.[37,38]

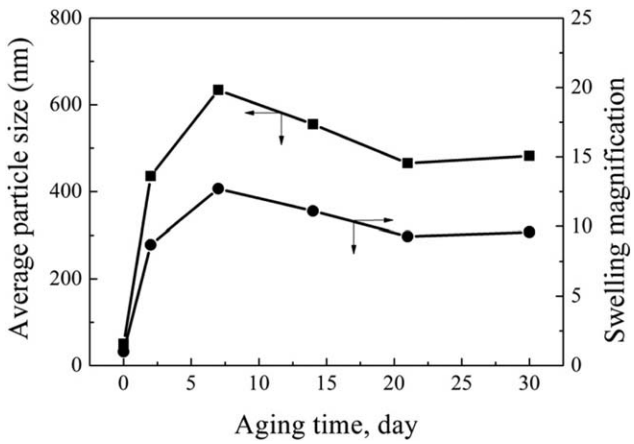

Figure 5. Particle size parameters of APMS after being swollen in brine.

Filtration Property

The weight of filtrates through a microporous membrane filter versus filtration time was measured. The filtration curves are shown in Figure 7 and they can be divided into two stages. One is the original rapid flow stage, and the other is the slow flow stage or sealing stage. The former stage means that the swollen microspheres have hardly time to bridge and block off the micropore, while the latter one implies bridging and plugging occur under pressure, owing to the high plugging strength and the cumulative effect of particles. In addition, the corresponding filtration parameters are listed in Table IV. The plugging factor, f, means the composition content of microspheres participating in plugging per unit volume, which could be derived from equation $Y = (1/\ln(1/(1-f))) \cdot \ln(1+v_0 \cdot X \cdot \ln(1/(1-f)))$ based on the nonlinear curve fitting analysis. Suppose f value approaches to 1.0, it expresses the membrane is completely blocked by microspheres and no filtrate passes through the micropores. The f values are 0.317, 0.236, and 0.306 for 7 days, 14 days, and 30 days, respectively, and show somewhat variance.

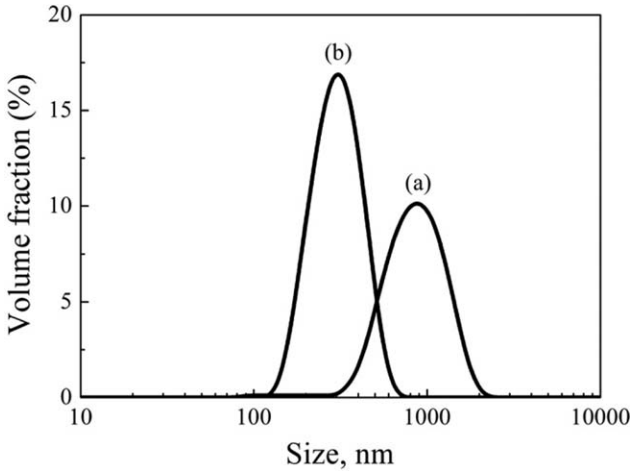

Figure 6. Particle volume fraction of APMS aged for 7 days (a) before and (b) after filtration.

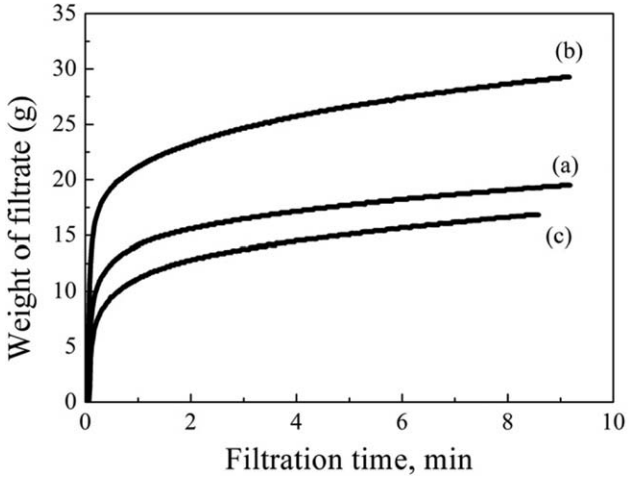

Figure 7. Filtration curves of APMS aged for (a) 7 days; (b) 14 days, and (c) 30 days.

It also confirms that APMS have good heat- and salinity-resistant properties.

However, it must be pointed out that the flow rate (v_0 value) at the original rapid flow stage is quite different from each other. The higher the v_0 value, the faster the flow speed is. The highest v_0 value appears after 14 days of aging. After hydration and aging for enough time, the microspheres become softer and easily to deform and pass through the microporous membrane filter, as well as blocking and bridging easily, which is ascribe to the second flow stage. With the aging time prolonging, the average particle size further decreases and the number of particles involved in the bridging and plugging increases from 2 to 4. The disappearance of outer layer makes the rigid particle cores contact closely and interact with another. The inside crosslinking density and strength ultimately still endow the swollen particles with a better plugging effect.

Core Plugging Characterization

In order to further simulate and evaluate the migration and plugging properties of APMS in underground channels, the core plugging tests were performed for varied core permeability and aging time through brine slug-microspheres slug-brine slug. The

Table IV. Plugging Factor and Mechanism of APMS at Different Aging Time

				Plugging mechanism	
Aging time (d)	d_{APMS}[a] (nm)	v_0[b]	f[c]	d/D[d]	N[e]
7	634	479	0.317	0.53	2
14	555	995	0.236	0.46	3
30	482	142	0.306	0.40	3-4

[a] Average particle size.
[b] Flow rate at the original rapid flow stage.
[c] Plugging factor.
[d] Ratio of particle size and micropore diameter (1.2 μm).
[e] Number of particles involved in bridging and plugging.[39]

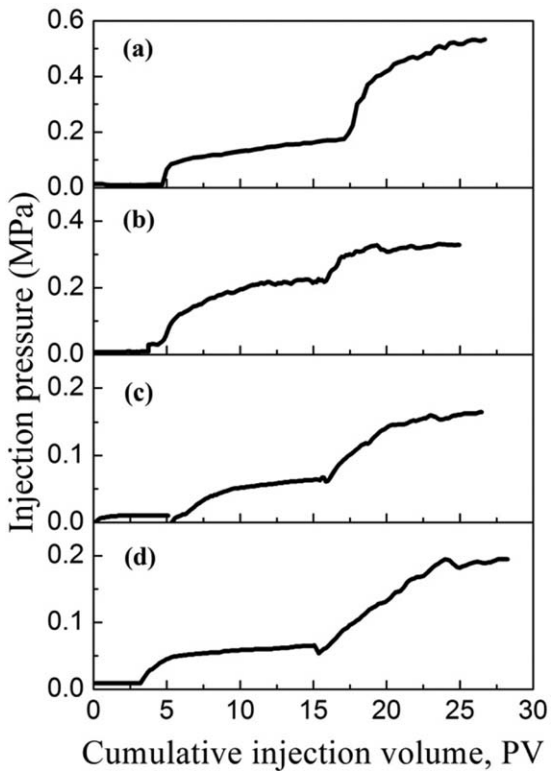

Figure 8. Core plugging pressure vary with injection volume under different core permeability and aging time: (a) 0.19 μm^2, 7 days; (b) 0.50 μm^2, 7 days; (c) 0.50 μm^2, 14 days; (d) 0.50 μm^2, 30 days.

curves of injection pressure versus cumulative injection volume are recorded in Figure 8. And the relative data containing injection pressure and resistance factor are summarized in Table V. The core used for plugging with 0.19 μm^2 of permeability has a higher porosity and a narrow pore throat, while the core with 0.50 μm^2 of permeability possesses a lower porosity and a double-size pore throat.

As shown in Figure 8, APMS can favorably enter and effectively plug the artificial cores with low and high permeability. The maximum pressure P_m recorded after the second injection of brine is nearly three times larger than the equilibrium pressure P_e after the microspheres/brine solution. So is the residual resistance factor F_{RR} in contrast to the resistance factor F_R. For the 0.19 μm^2 core, F_{RR} is up to 53.3 and far above F_R (17.5). Additionally, the injection pressure in the third growth period displays obvious fluctuations, presenting an alternate progress of deformation, breakthrough, and migration, bridging and plugging; while the relative pressure maintains for much injection volume, also illustrating well resistance to water flushing and good plugging strength.

Concretely speaking, according to previous theory,[40–42] there exist different penetrating mechanisms in core with different permeability. As to the core of 0.19 μm^2, the relationship of the particle size (d_{APMS}) and the pore throat ($2r_{pore\ throat}$) is 3 $d_{APMS} < 2r_{pore\ throat} < 10d_{APMS}$, displaying that the swollen particles can partially enter the core and form an internal cake, but the penetration depth is shallow. Due to the surface adsorption, mechanical capture, hydrodynamic effect and interactions

Table V. Core Plugging Information of APMS

Time (d)	k^a (μm^2)	φ^b (%)	$2r_{pore}{}^c$ (μm)	$3d_{APMS}{}^a$ (nm)	$10d_{APMS}{}^a$ (nm)	P_0 (MPa)	P_e (MPa)	P_m (MPa)	F_R	F_{RR}
7	0.19	26.0	4.84	1.90	6.34	0.010	0.175	0.533	17.5	53.3
7	0.50	16.1	9.96	1.90	6.34	0.013	0.220	0.329	16.9	25.3
14	0.50	15.8	10.06	1.67	5.55	0.010	0.067	0.165	6.7	16.5
30	0.50	15.9	10.04	1.45	4.82	0.009	0.065	0.195	7.2	21.7

[a] Permeability of artificial core.
[b] Porosity of core.
[c] Radius of the pore throat in core calculated by the formula: $(8\ k/\varphi)^{0.5}$.

between particles, some microspheres are destined to be retained on pore surfaces or captured in smaller pore throat.[25] So the subsequent injection pressure is relatively high and grows constantly and the platform is not obvious in the test range [Figure 8(a)]. As to the core of 0.50 μm^2, in despite of the aging time, the relational expression is $2r_{pore\ throat} > 10d_{APMS}$, meaning that the particles can be easily injected and smoothly transported in the core without much impediment. Correspondingly, the relative lower injection pressure and a distinct plateau are produced [Figure 8(b–d)]. In a word, the aforesaid results imply that at higher permeability, the swollen microspheres migrate easily into deeper location of core under pressure and still play a role in plugging again by bridging.

Moreover, comparatively, P_e, P_m, F_R, and F_{RR} values of APMS at 0.19 μm^2 are all greater than those values at 0.50 μm^2 under the same aging time. This also indicates that in a certain range, the smaller the pore throat, the greater the required pressure difference to push the colloid through pore throat, and the better the plugging effect.[25,43] Here, lowering the core permeability (k) or the pore throat size ($2r_{pore}$) is same as increasing the particle size, which is related to the increased plugging.[44] However, in order to obtain a deep profile control, the size of the swollen particles must be kept within an appropriate range. For a given pore throat, a deeply controlling profile and a particle with suitable size should be taken into overall account. In this study, the swollen microspheres could pass through the pore throat and effectively plug the core.

Besides, with the improvement of aging time, P_e and F_R values change little while F_{RR} values show a totally declined tendency. This is also coincident with the results discussed in the swellability and filtration characterization sections. The size of microspheres increases firstly and then decrease to a balanced state. A great number of microspheres in a bridge cause compaction and resistance to water flow, providing a way to plug large pore throat. Meanwhile, the outer layer of particles gradually hydrates, softens and disappears, but they still possess good crosslinking strength, due to the rigid particles contacting and interacting. All of those are inseparably related to the special groups and cross-linking structures of APMS as well as the strong cationic-anionic interaction between microspheres. All in all, the good anti-heat, anti-salinity and plugging performances of APMS after aging are attributable to the comprehensive effect of the above factors.

CONCLUSIONS

Heat- and salinity-resistant amphiprotic polyacrylamide microspheres were synthesized and their performances were characterized. Five monomeric units and uniform structures endow the particles with suitable swellability, heat-resistance and salinity-resistance properties under high temperature and TDS for a long-term aging, which are before those of the current product. Furthermore, the favorable membrane filtration and plugging performances are also attributed to the combined action of the interaction of designed structures, the deformability after aging, the rigid crosslinking inner cores, and the bridging and block-off abilities. All of those mean that the designed copolymer microspheres have a potential superiority in applying in the oilfield for water shutoff and profile modification. Successful core flood example shows that the copolymer microspheres can be used for high salinity high temperature reservoir to plug the high permeable layers. The new method using copolymer microspheres broadens the potential application of EOR processes to target oil reservoirs.

ACKNOWLEDGMENTS

The authors thank the staff of Sinopec Zhongyuan Oilfield Branch and the reviews for their helpful discussions and suggestions.

REFERENCES

1. Sheng, J. J. Modern Chemical Enhanced Oil Recovery: Theory and Practice. Gulf Professional Publishing, **2011**.
2. Han, D. K.; Yang, C. Z.; Zhang, Z. Q.; Lou, Z. H.; Chang, Y. I. *J. Pet. Sci. Eng.* **1999**, *22*, 181.
3. Li, G.; Zhai, L.; Xu, G.; Shen, Q.; Mao, H. *J. Dispers. Sci. Technol.* **2000**, *21*, 367.
4. Avendano, J.; Pannacci, N.; Herzhaft, B.; Gateau, P.; Coussot, P. *Oil Gas Sci. Technol. Rev. IFP Energies Nouvelles* **2012**, *67*, 921.
5. Vermolen, E. C. M.; van Haasterecht, M. J. T.; Masalneh, S. K.; Faber, M. J.; Boersma, D. M.; Gruenenfelder, M. SPE 141497, SPE Middle East Oil and Gas Show and Conference, Manama, Bahrain, **2011**; Vol. *1*, p 25.
6. Levitt, D. B.; Pope, G. A. SPE 113845, SPE Symposium on Improved Oil Recovery, Tulsa, Oklahoma, **2008**; Vol. *1*.
7. Wever, D. A. Z.; Picchioni, F.; Broekhuis, A. A. *Prog. Polym. Sci.* **2011**, *36*, 1558.
8. Taylor, K. C.; Nasr-El-Din, H. A. *J. Pet. Sci. Eng.* **1998**, *19*, 265.
9. Shi, L. T.; Li, C.; Zhu, S. S.; Xu, J.; Sun, B. Z.; Ye, Z. B. *J. Chem.* **2013**, *2013*, 1.
10. Pancharoen, M. Physical Properties of Associative Polymer Solutions. A Thesis of Stanford University, **2009**.

11. Chauveteau, G.; Omari, A.; Tabary, R.; Renard, M.; Rose, J. SPE 59317, Proceedings of SPE/DOE Improved Oil Recovery Symposium, Tulsa, OK, **2000**; Vol. *1*, p 3.
12. Chauveteau, G.; Tabary, R.; Renard, M.; Omari, A. SPE 50752, SPE International Symposium on Oilfield Chemistry, Houston, TX, **1999**; Vol. *1*, p 16.
13. Sydansk, R.; Xiong, Y.; Al-Dhafeeri, A.; Schrader, R.; Seright, R. *SPE Prod. Facilities* **2005**, *20*, 240.
14. Muruaga, E.; Flores, M. V.; Norman, C.; Romero, J. SPE 113334, SPE Symposium on Improved Oil Recovery, Tulsa, OK, **2008**; Vol. *1*, p 19.
15. Wu, Y. S.; Bai, B. SPE 115678, SPE Annual Technical Conference and Exhibition, Denver, CO, **2008**; Vol. *1*, p 21.
16. Yu, H.; Wang, Y.; Ji, W.; Zhang, J.; Zhang, P.; Li, K.; Wang, S. *Pet. Sci. Technol.* **2011**, *29*, 715.
17. Zaitoun, A.; Tabary, R.; Rousseau, D.; Pichery, T.; Nouyoux, S.; Mallo, P.; Braun, O. SPE 106042, SPE International Symposium on Oilfield Chemistry, Houston, Texas, **2007**; Vol. *1*.
18. Bai, B.; Wu, Y.; Shuler, P. A First Annual Report of Missouri University of Science and Technology, **2009**.
19. Dai, C.; Zhao, G.; Zhao, M.; You, Q. *Molecules* **2012**, *17*, 14484.
20. Yao, C.; Lei, G.; Li, L.; Gao, X. *Energy Fuels* **2012**, *26*, 5092.
21. Sydansk, R. D.; Smith, T. B. SPE 17383, SPE Enhanced Oil Recovery Symposium, 20 April, Tulsa, OK, **1988**.
22. Smith, J. E. SPE 28989, SPE International Symposium on Oilfield Chemistry, San Antonio, TX, **1995**; p 461.
23. Pritchett, J.; Frampton, H.; Brinkman, J. SPE 84897, SPE International Improved Oil Recovery Conference in Asia Pacific, **2003**; p 1.
24. Frampton, H.; Morgan, J. C.; Cheung, S. K. SPE 89391, SPE/DOE Symposium on Improved Oil Recovery, Tulsa, **2004**; p 1.
25. Yao, C.; Lei, G.; Cathles, L. M.; Steenhuis, T. S. *Environ. Sci. Technol.* **2014**, *48*, 5329.
26. Sanchez, J. C.; Martiaez, A.; Ortega, P. *Polym. Bull.* **2006**, *56*, 437.
27. Wan, T.; Wang, L.; Yao, J. *Polym. Bull.* **2008**, *60*, 431.
28. Lin, M.; Dong, Z.; Peng, B.; Li, M.; Wu, Z. *Acta Polym.* **2011**, *11*, 48.
29. Zhao, H.; Wu, Z.; Zheng, X.; Lin, M.; Li, M. *Fine Chem.* **2005**, *22*, 62.
30. Han, X.; Li, M.; Guo, J.; Lin, M.; Wu, Z. *J. China Uni. Pet.* **2008**, *32*, 127.
31. Chen, Q.; Xu, J.; Wang, C.; Ge, C.; Wu, Y. *J. Chem. Eng. Chin. Univ.* **2007**, *21*, 705.
32. Liu, M. H. Preparation and Application of Organic Polymer Flocculant. Beijing Chemistry Industry Press, **2006**.
33. Lin, M.; Han, F.; Li, M.; Wu, Z. *Membr. Sci. Technol.* **2003**, *23*, 11.
34. Sun, Y.; Saleh, L.; Bai, B. *Rheology* **2012**, *8*, 187.
35. Valle, H.; Rivas, B. L.; Aguilar, M. R.; Roman, J. S. *J. Appl. Polym. Sci.* **2013**, *129*, 537.
36. Yu, Z. S.; Xia, Y. M. *Special Petrochem.* **2012**, *29*, 79.
37. Kiatkamjornwong, S.; Phunchareon, P. *J. Appl. Polym. Sci.* **1999**, *72*, 1349.
38. Li, G.; Zhang, G.; Wang, L. *Energy Fuels* **2013**, *27*, 6632.
39. Lin, M.; Dong, Z.; Han, F.; Li, M.; Wu, Z. *Membr. Sci. Technol.* **2005**, *25*, 42.
40. Maroudas, A. *Filtr. Sep.* **1966**, *3*, 115.
41. Pautz, J. F.; Crocker, M. E.; Walton, C. G. SPE 18888, SPE Production Operations Symposium, Oklahoma City, Oklahoma, **1989**.
42. Hong, S. D. Physical Basis of Reservoir; Beijing Petroleum Industry Press, **1985**.
43. Lei, G. New technology of deep profile control and displacement of pore throat scale elastic microspheres. China University of Petroleum Press, **2011**.
44. Veerapen, J. P.; Nicot, B.; Chauveteau, G. A. SPE 68962, SPE European Formation Damage Conference, Hague, Netherlands, **2001**.